

This article was downloaded by:[Wylie, B. K.]
On: 27 May 2008
Access Details: [subscription number 793295431]
Publisher: Taylor & Francis
Informa Ltd Registered in England and Wales Registered Number: 1072954
Registered office: Mortimer House, 37-41 Mortimer Street, London W1T 3JH, UK



International Journal of Digital Earth

Publication details, including instructions for authors and subscription information:
<http://www.informaworld.com/smpp/title~content=t777764757>

Integrating modelling and remote sensing to identify ecosystem performance anomalies in the boreal forest, Yukon River Basin, Alaska

B. K. Wylie ^a; L. Zhang ^a; N. Bliss ^a; L. Ji ^a; L. L. Tieszen ^b; W. M. Jolly ^c

^a SAIC, USGS Earth Resources Observation and Science (EROS) Center, Sioux Falls, SD, USA

^b USGS EROS Center, Sioux Falls, SD, USA

^c USDA Forest Service, Fire Sciences Laboratory, Missoula, MT

Online Publication Date: 01 January 2008

To cite this Article: Wylie, B. K., Zhang, L., Bliss, N., Ji, L., Tieszen, L. L. and Jolly, W. M. (2008) 'Integrating modelling and remote sensing to identify ecosystem performance anomalies in the boreal forest, Yukon River Basin, Alaska', International Journal of Digital Earth, 1:2, 196 — 220

To link to this article: DOI: 10.1080/17538940802038366

URL: <http://dx.doi.org/10.1080/17538940802038366>

PLEASE SCROLL DOWN FOR ARTICLE

Full terms and conditions of use: <http://www.informaworld.com/terms-and-conditions-of-access.pdf>

This article maybe used for research, teaching and private study purposes. Any substantial or systematic reproduction, re-distribution, re-selling, loan or sub-licensing, systematic supply or distribution in any form to anyone is expressly forbidden.

The publisher does not give any warranty express or implied or make any representation that the contents will be complete or accurate or up to date. The accuracy of any instructions, formulae and drug doses should be independently verified with primary sources. The publisher shall not be liable for any loss, actions, claims, proceedings, demand or costs or damages whatsoever or howsoever caused arising directly or indirectly in connection with or arising out of the use of this material.

Integrating modelling and remote sensing to identify ecosystem performance anomalies in the boreal forest, Yukon River Basin, Alaska

B.K. Wylie^{*a}, L. Zhang^a, N. Bliss^a, L. Ji^a, L.L. Tieszen^b and W.M. Jolly^c

^aSAIC, USGS Earth Resources Observation and Science (EROS) Center, Sioux Falls, SD 57198, USA. Work performed under USGS contract 03CRCN0001; ^bUSGS EROS Center, Sioux Falls, SD 57198, USA; ^cUSDA Forest Service, Fire Sciences Laboratory, Missoula, MT, 59808

(Received 30 October 2007; final version received 1 February 2008)

High-latitude ecosystems are exposed to more pronounced warming effects than other parts of the globe. We develop a technique to monitor ecological changes in a way that distinguishes climate influences from disturbances. In this study, we account for climatic influences on Alaskan boreal forest performance with a data-driven model. We defined ecosystem performance anomalies (EPA) using the residuals of the model and made annual maps of EPA. Most areas (88%) did not have anomalous ecosystem performance for at least 6 of 8 years between 1996 and 2004. Areas with underperforming EPA (10%) often indicate areas associated with recent fires and areas of possible insect infestation or drying soil related to permafrost degradation. Overperforming areas (2%) occurred in older fire recovery areas where increased deciduous vegetation components are expected. The EPA measure was validated with composite burn index data and Landsat vegetation indices near and within burned areas.

Keywords: climate change; anomaly; performance; boreal; Alaska; Yukon River

Introduction

Site conditions, changing climate, natural disturbances, and the effects of human management are often intermingled to create complex responses in vegetation. Monitoring methods that do not separate these influences are difficult to interpret.

We present a method for analysing ecosystem performance anomalies that separates the influences of climate and site potential (a measure of the land's inherent productivity) from the influences of disturbances, and we show its application to boreal forest ecosystems in the Yukon River Basin, Alaska. The method builds upon remotely sensed measures of vegetation greenness for each growing season. However, a time series of greenness inherently reflects annual variations in temperature and precipitation. The method presented here seeks to remove the influence of climate, so that changes in underlying ecological condition are highlighted. We define an 'expected ecosystem performance' to represent the greenness response expected in a particular year given the climate of that year, and we distinguish 'performance anomalies' as cases where the ecosystem response is significantly different than the expected ecosystem performance.

*Corresponding author. Email:wylie@usgs.gov

High northern latitudes are experiencing climate change at faster rates than other parts of the globe (Corell 2006, Hassol 2004). This warming has the potential to create positive feedbacks, which could accelerate warming trends and intensify impacts on arctic ecosystems (Chapin *et al.* 2005, Foley 2005, Hinzman *et al.* 2005, Walker 2007). In its traditional range, the greenness of boreal forests has been decreasing, as measured by satellite vegetation indices (Goetz *et al.* 2005, Bunn and Goetz 2006, Reed 2006). This decrease is partially related to increasing fires, and larger and more frequent fires are anticipated (Rupp *et al.* 2000a), which will affect carbon storage (Harden *et al.* 2000). The deciduous components of boreal forests are likely to increase because of postfire succession (Rupp *et al.* 2000a, Goulden *et al.* 2006) and other climate change impacts (Kronberg and Watt 2000, Calef *et al.* 2005). Changing permafrost and active layer thickness will affect boreal ecosystems (Hinkel and Nelson 2003, Bunn *et al.* 2005, Jorgenson *et al.* 2006, Zimov *et al.* 2006) through changes in both surface and subsurface moisture (Yoshikawa and Hinzman 2003, Striegl *et al.* 2005, Buffam *et al.* 2007, Smith *et al.* 2007). Under extreme conditions, critical boreal forest ecological thresholds could be exceeded, resulting in conversion to a persistent grassland steppe (Rupp *et al.* 2000b).

Identification of 'climate change hot spots' (Giorgi 2006) or 'environments at risk' (Saxon *et al.* 2005) is important at regional and local scales. Areas under stress are vulnerable to significant changes in vegetation (Rupp *et al.* 2000b, Calef *et al.* 2005, Hinzman *et al.* 2005). Quantification of these anomalous areas will also be useful for regional carbon modelling (Magnani *et al.* 2007), wildlife dynamics (Herfindal *et al.* 2006), and future vegetation predictions.

Annual variations in climate affect boreal forest biomass production (Kang *et al.* 2005, Kimball *et al.* 2006, Dunn *et al.* 2007) and plant growth (Bunn *et al.* 2005). Several methods have been used to understand how climate or site conditions influence the normalised difference vegetation index (NDVI) response. Hermann *et al.* (2005) and Wessels *et al.* (2007) used regression approaches to account for climatic impacts on NDVI in Africa to reveal anomalies attributable to factors other than climate. Similar approaches have been used with grasslands and steppes in North America (Wylie *et al.* 2005). Regression tree methods have been used to quantify topographic controls on interannual vegetation variability (White *et al.* 2005) and to map maximum NDVI from meteorological data (Schwabacher and Langley 2001). Seasonal NDVI was predicted for Canadian boreal forests using a random forests ensemble prediction (Bunn *et al.* 2005).

Methods

Our modelling approach has four steps:

1. Compute ecosystem performance (EP) in terms of a seasonally integrated NDVI.
2. Compute an expected ecosystem performance, representing the ecosystem performance that would be expected for each pixel given that it had not burned in 25 years and given the site potential and climate in the respective year.

3. Compute an ecosystem performance anomaly as the difference between the ecosystem performance and the expected ecosystem performance.
4. Evaluate the changes in the ecosystem performance anomaly over time.

The ecosystem performance measure (step 1) reflects the actual ecosystem performance for each pixel, thus it incorporates many influences including climate, site potential, ecosystem stresses, and land management. The expected ecosystem performance measure (Step 2) excludes the influences of ecosystem stresses (such as fire or insects) and land management (such as logging or overgrazing), and incorporates the site potential and climate (the precipitation and temperature patterns of the given year). The measure of ecosystem performance anomaly (step 3) highlights differences between the actual (step 1) and expected (step 2) ecosystem performance measures, so that a negative value indicates an ecosystem that is underperforming (perhaps due to fire or insects) and a positive value indicates an ecosystem that is overperforming. Trends in the ecosystem performance anomaly (step 4) give insights into the presence of ecosystem stresses or changes in land management and will enable land managers and policy makers to evaluate the condition of ecosystems over large areas, detect significant degradation or improvement, and evaluate the effects of policies on ecosystem performance.

The following sections give details on the operational definitions and application of the methods to the boreal forest.

Piecewise regression techniques

Several of the steps in the modelling process make use of rule-based piecewise regression techniques. The piecewise regression approaches first partition the information space into subspaces to optimise prediction. Then a linear multiple regression model is fit within each information subspace. The methods allow more precise modelling of complex nonlinear systems than standard multiple regression and provide understanding of the mechanisms that control the relationships between the independent and dependent variables. We applied rule-based piecewise regression modelling methods (Wylie *et al.* 2007) to predict site potential and expected ecosystem performance, as prototyped by Zhang *et al.* (2006). A subset of input variables was selected to reduce model complexity and improve model robustness (Lauenroth *et al.* 2006). We took care to ensure that the variables selected by the modelling process were biologically meaningful.

Ecosystem performance (EP)

We presently define ecosystem performance (EP) in terms of seasonal integrated NDVI over a growing season. Ecosystem performance was introduced by Tieszen *et al.* (1997) and represents vegetation dynamics as captured by the seasonal integrals of NDVI. Jia *et al.* (2002) and Breshears *et al.* (2005) have used seasonal integrals of NDVI as proxies for vegetation dynamics. Prince *et al.* (1991) and Xia *et al.* (2005) used seasonally integrated NDVI to map biomass, and Knapp and Smith (2001) used annual NDVI integrals as a proxy for net primary production (NPP). Goetz *et al.* (2005) combined photosynthetically active radiation and NDVI as a proxy for gross photosynthesis in boreal forests. Acknowledging that there are errors associated in the conversion of NDVI to biomass, gross primary productivity, or NPP, we choose to

use the growing season integral of NDVI as a proxy for EP, ensuring that EP is a quantity that can be consistently produced in both space and time.

$$EP = \text{growing season integrated NDVI} \quad (1)$$

We used 1 km resolution advanced very high resolution radiometer (AVHRR) NDVI from 1995 to 2004. These NDVI data were corrected for atmospheric, wide field-of-view, and georegistration effects, and composited into 7-day periods (Eidenshink 2006). The sequence of 7-day NDVI images was temporally smoothed to remove residual clouds (Swets *et al.* 2000). A baseline NDVI value of 0.09 associated with bare soil and dormant vegetation was subtracted from the NDVI composites (Jia *et al.* 2006), and the remainder was summed for the period from April through the first week of October. This growing season time integrated NDVI served as an estimate of ecosystem performance for the boreal forest area in our study. Goetz *et al.* (2005) found little difference between integration periods from May to September and May to October for North American boreal forests; however, our integration began earlier and was focused only on higher latitude boreal forests in the Yukon River Basin.

Expected ecosystem performance (EEP)

Expected ecosystem performance (EEP) is the EP that can be expected on a given site and for climatic conditions of a given year, in the absence of disturbance. Highly productive sites will have higher ecosystem performance measures than sites with poor soils, steep slopes, or other conditions not conducive for vegetation growth. We incorporate the site potential in the measure of EEP, so that pixels that have poor site conditions will have lower EEP than those with good site conditions. In a similar way, years that have favorable climate conditions will have higher EEP than those with unfavorable conditions (too hot or too cold, or too wet or too dry).

We define EEP using a piecewise regression model predicting EP on undisturbed sites (sites not burned in 25 years), driven by the site potential and yearly climate variables:

$$EEP = f(\text{site potential, land cover, yearly climate})_{\text{undisturbed}} \quad (2)$$

Ideally, a map of site potential would be derived from data sources that are independent of the remotely sensed data that is used for estimating EP. However, such maps were not available for our study area, so we developed a method for mapping site potential from remotely sensed and ancillary data.

Our model does not account for forest age effect, although this effect may slightly influence the modeled ecosystem performance anomaly (section 2.4) results. Chen *et al.* (2003) documented that black spruce NPP in Canada is nonlinearly related to forest stand age with approximate 50-year-old stands having the highest NPP. However, we consider the forest age effect is minor relative to disturbances, thus the age effect is accounted for in the model error.

Site potential

Site potential represents the long-term EP that averages out climatic variations but accounts for spatial variation in long-term EP associated with site conditions like

drainage, elevation, slope and aspect, permafrost conditions, soils, domain clusters (Saxson *et al.* 2005), and surface geology. Site potential does not include disturbance effects. The site potential map was developed at 1 km resolution to account for the important effects of elevation, slope, aspect (Viereck *et al.* 1992, Calef *et al.* 2005), and growing season length. Saxson *et al.* (2005) developed a good approximation of site potential which combined the effects of climate, soils, and topography.

We developed a site potential map for boreal forest using long-term (1995 to 2004) average seasonal integrated NDVI as a preliminary estimate of site potential. To make the site potential map independent of recent disturbance, we excluded areas that had burned within the previous 25 years. Measures of vegetation productivity in boreal forest systems (e.g., NDVI, gross primary productivity, and net primary productivity) show recovery within 25 years after a fire (Viereck and Van Cleve 1984, Hicke *et al.* 2003, Epting and Verbyla 2005, Karjalainen 2005, Goulden *et al.* 2006).

We used temporally static spatial data sets to train piecewise regression models (using Cubist software[®]: <http://www.rulequest.com/>) to estimate long-term average seasonal integrated NDVI. To construct the model, 1600 random points were cast on coniferous forest regions from the modified 1991 land cover map within the Yukon River Basin. A database was constructed from the random points that had not burned in the previous 25 years with attributes for land cover, ecoregion, domain cluster, permafrost, elevation, north and south aspect, surface geology, and long-term average seasonal integrated NDVI:

$$\text{Site Potential} = f(\text{land cover, ecoregion, domain clusters, permafrost, elevation and derivatives, surface geology}) \quad (3)$$

This model showed biases with too much emphasis on the more common values near the average. To remedy the biases, a bagging approach was applied (DeFries and Chan 2000). The random points were split into two groups: 1) those within one standard deviation of the long-term average seasonal integrated NDVI and 2) those higher or lower than the one standard deviation limits. A subset training data set was developed by combining a random sample of 35% of the values in group 1 with a random sample of 75% of the values in group 2. The new data set provided a model development data set that gave roughly equal representation to the rarer extremely high or low values and the more common values near the mean. A piecewise regression model was developed from this data set and applied to produce a map. This process was repeated three times with replacement and resulted in three different site potential maps. Using a bagging approach, the average prediction from the three maps was used as the final site potential map.

Climate

Climate data were developed according to the methods of Jolly *et al.* (2005) and interpolated on a 5-km grid. Maps of monthly surface radiation, precipitation, and minimum and maximum temperatures were resampled to 1-km resolution using bilinear interpolation to match the AVHRR NDVI data sets. Seasonal periods were early summer (May–June), late summer (July–August), fall (September–October),

and winter (November–April). Sixteen climate variables were formed by averaging the four climate characteristics for each of the four seasonal periods.

Land cover data

A land cover data set for 1991 was available from the Forest Health Monitoring Clearinghouse (<http://agdc.usgs.gov/data/projects/fhm>), developed from AVHRR data for 1991. We used decision tree methods to fill in five coniferous forest land cover classes within the areas classed as 1991 fires. High latitude boreal forests often are quite open forests with significant shrub and tundra vegetation interspersed. Several of the selected coniferous forest classes used in this analysis also had secondary components of deciduous trees as well.

The land cover data set for 1991 from the Forest Health Monitoring Clearinghouse (<http://agdc.usgs.gov/data/projects/fhm>) was developed using AVHRR data for 1991, but we needed a representation of the long-term areas of forest, whether burned or not. We used decision tree methods to fill in five coniferous forest classes within the areas classed as 1991 fires. This was done using a boosted decision tree model (See5 software, De'ath and Fabricius 2000, DeFries and Chan 2000) trained on unburned areas (13 784 random points) with temporally static data layers, including ecoregions, domain clusters, elevation, north and south aspect, compound topographic index (CTI), permafrost, surface geology, and site potential (developed in this study). These site characteristics have been good indicators of expected forest types (Viereck and Van Cleve 1984, Calef *et al.* 2005). The boosted decision tree model had an overall training accuracy of 98% on 13 784 observations. Some minor manual refinements were made within the 1991 burns using heads up digitizing. Only areas with coniferous forests within the Yukon River Basin were used in this analysis.

Other data

Unified EcoRegions (Nowacki *et al.* 2001, <http://agdc.usgs.gov/data/projects/fhm>) were used for ecoregion delineation and were represented as a categorical variable in the database. The permafrost layer was from the 1:2 500 000 Permafrost map of Alaska (Ferrians 1965, <http://agdcftp1.wr.usgs.gov/pub/projects/fhm/permafrost.html>), and was also used as a categorical variable. Surface geology was also a categorical variable, mapped at 1:1 584 000 (Karlstrom *et al.* 1964). Elevation was from a 1-km digital elevation model (DEM). The DEM derivatives were calculated from 60-m DEMs and consisted of a compound topographic index (CTI) and north and south aspects with steep slopes. The CTI is a function of both slope and upstream contributing area (Beven and Kirkby 1979, Chaplot and Walter 2003). North aspects were defined as aspects between 315° and 45° (where North = 0° and aspect angles are measured clockwise) on slopes greater than 8.5%. South aspects were defined as aspects between 135° and 225° on slopes greater than 8.5%. East and West aspects were disregarded. These DEM derivatives were continuous variables that averaged the CTI or the measured percent occurrence of the aspect variables for each 1-km resolution grid cell. Environmental domains represent areas with similar environmental conditions and were derived by Saxon *et al.* (2005) by clustering edaphic, topographic, and climatic information. Fire perimeters and burn dates were

acquired from the Bureau of Land Management fire database (<http://agdc.usgs.gov/data/blm/fire>).

Model for expected ecosystem performance (EEP)

The model for EEP as shown in equation (2) was developed by applying a rule-based piecewise regression technique. The training data used EP as the predicted variable, and site potential and climate as the driving variables. The model was trained on a subset of the random points in the boreal forest area for locations that had not burned in the previous 25 years. The training database included annual EP and climate data for the years 1995 to 2004 (excluding 2000), as well as forest type land cover. Piecewise regression models were developed to predict EEP for all years from this database using the independent variables, including site potential, seasonal integrals (early summer, late summer, fall and winter) of minimum temperature, maximum temperature, precipitation, and solar radiation, and land cover for boreal forest classes. Three bagging models were derived using methods similar to the site potential modelling, but in this case, the same input variables were used in all three bagging models.

Ecosystem performance anomaly (EPA)

We define an ecosystem performance anomaly (EPA) as the ecosystem performance measure in a given year minus the expected ecosystem performance:

$$\text{EPA} = \text{EP} - \text{EEP} \quad (4)$$

We assume that the influence of climate will be the same for both EP and EEP, so that the ecosystem performance anomalies are not associated with annual variations in climate.

In Figure 1, the EEP is plotted against EP. The scatter of the points around the overall regression line represents the EPA. We assume that most of the variation of the residuals around the regression line represents information about anomalous ecosystem performance. The residuals also include model error, but we expect it to be small relative to the performance anomaly information and largely accounted for by the confidence intervals. Anomaly thresholds were determined from the 90% confidence intervals calculated when fitting a regression model between EP and EEP. Annual anomaly maps were computed using the difference between EP and EEP for each year.

We conducted validation studies on the EPA measure using composite burn index data and Landsat data.

Trends in ecosystem performance anomaly

We evaluate trends in EPA by determining if there is a statistically significant positive or negative slope to a regression fit through the EPA measures across time. By analysing each pixel, we can make maps of the trends.

We define an ecosystem performance anomaly trend (EPAT) in terms of a linear regression for each pixel, where the time (year) is the independent variable and the EPA is the dependent variable:

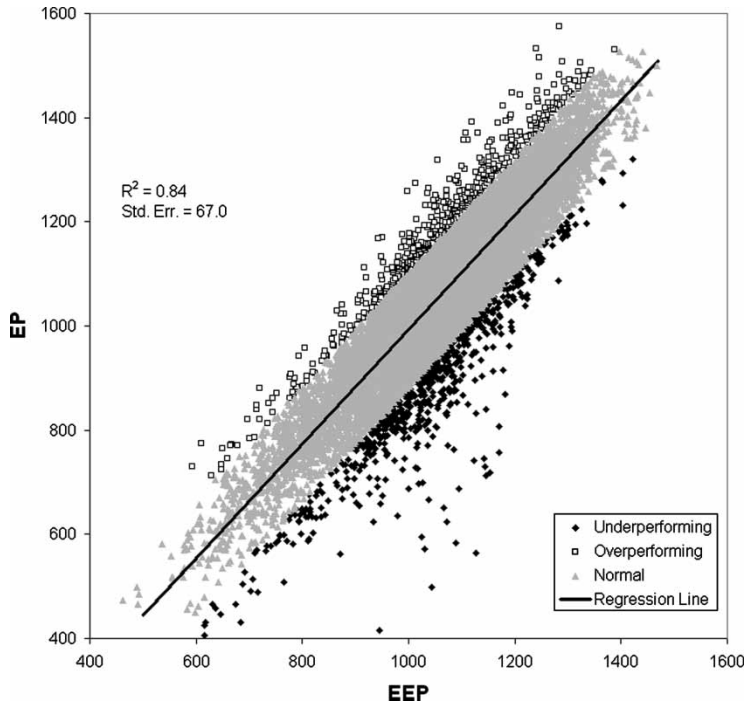


Figure 1. Model predictions of expected ecosystem performance (EEP) compared with actual ecosystem performance (EP) for 1995–2004 (excluding 2000). Pixels were selected randomly from boreal forest areas which have not burned in 25 years. Green areas represent overperformance and are greater than the 90% confidence limit above the regression line. Magenta areas represent underperformance, and are less than the 90% confidence limit below the regression line.

$$\text{EPA} = a \times \text{year} + b \quad (5)$$

where a is the slope of the regression line, and b is the intercept. We classify all pixels according to whether the slope is statistically significant and whether the slope is positive, near zero, or negative. The annual trend of the performance anomaly measure should reveal areas which are degrading or improving over time, with climatic variation taken into account.

The performance anomaly time series (1996–1999, 2001–2004) was assessed with a time series regression. The year 2000 was not used because of unreliable AVHRR data owing to the degraded orbit and late overpass time of the NOAA 14 satellite. Linear regressions were constructed with ‘year’ as the independent variable and ‘ecosystem performance anomaly’ as the dependent variable. This analysis was done for all the boreal forest pixels in the study area. The spatial output included the estimated EPA value, n (number of years), slope coefficient, standard error, and t score. For this analysis, the map of t score was used to identify both slope significance and slope direction (positive or negative).

The sequence of EPA maps was summarised to show areas with consistent EPA through the time period. Areas which were identified as underperforming anomalies for at least 75% of the years or overperforming for at least 75% of the years were

identified. This temporal summarisation of EPA was then combined with EPAT to identify combinations of EPAT and areas of consistent EPA.

Results

Expected ecosystem performance

The important driving variables for EEP were site potential, land cover (five forest classes), maximum temperature (Sept.–Oct.), minimum temperature (May–June, July–August, winter), precipitation (all seasons), and photosynthetically active radiation (all seasons). The same variables were used for each of the three randomised subsets, and the model had training R^2 values ranging from 0.81 to 0.90. The test data were the subset of the data not used for training. Because the training data were stratified to give a more equal representation throughout the range of EP values, the test data were greatly restricted in high and low values of EP, and a high proportion were near the mean EP values. Because the R^2 statistic is sensitive to both the range of values and their distributions, lower R^2 are observed on the test data. Values of the mean standard error (MSE) of the regression were similar for the test and training data sets, with the test MSE values being lower. The average predicted values from the three models for computing EEP showed little bias and accounted for 84% of the variation of EP (Figure 1).

The piecewise regression models for each of the three bagging models used a committee model of five which resulted in 15 piecewise regression models. A committee model builds a set of successive piecewise regression models with each successive model improving on the errors of the previous model (<http://www.rulequest.com/cubist-win.html>). Committee models are useful for fine tuning reasonably accurate models and for producing maps which are more spatially coherent than noncommittee models. Each of the three bagging models had an average of 33 piecewise regression equations for each of the five committee models. The result was an overall total of 500 piecewise regression equations each with different combinations of independent variables and stratification criteria. In other studies, we have quantified the relative frequency of use and importance for prediction of variables from complex piecewise regression models (Wylie *et al.* 2007, Wylie *et al.* 2003, Zhang *et al.* 2007). The variable use-frequency for gratifying piecewise regressions was quantified as the percent utilisation. Similarly, a nonlinear “prediction importance” weight was determined for each regression equation and summed across the regression equations. Variables important for stratification of the various regressions were land cover, site potential, fall solar radiation, and late summer precipitation (Table 1). As a result, important independent variables in the regression models were spring minimum temperature, site potential, fall maximum temperature, fall solar radiation, and late summer solar radiation. These models were used for mapping EEP for each year from 1995 to 2005 for coniferous boreal forest areas within the Yukon River Basin.

Ecosystem performance anomaly

Maps of the EPA are shown in Figure 2. The anomaly maps were coloured to reflect negative anomalies (underperforming), positive anomalies (overperforming), and normal pixels as determined by the 90% confidence intervals from Figure 1.

Table 1. Relative use and relative prediction importance of independent variables for the EEP model.

Independent variable	Stratification relative use (%)	Prediction importance (%)
Site potential	15%	11%
Fall solar radiation	14%	7%
Late summer precipitation	14%	6%
Late summer minimum temperature	4%	15%
Winter solar radiation	10%	6%
Land cover	16%	0%
Fall maximum temperature	6%	9%
Spring minimum temperature	2%	13%
Late summer solar radiation	5%	7%
Winter precipitation	5%	4%
Spring solar radiation	2%	8%
Spring precipitation	4%	5%
Winter minimum temperature	3%	5%
Fall precipitation	1%	3%

Figure 3 shows the performance anomaly map for 2004, with an overlay of recent fire perimeters. The negative values for the performance anomalies often indicate that vegetation is underperforming in areas with recent fires. Underperforming areas which were not burned are also of interest as they may represent areas of insect infestations or changing soil and permafrost conditions which result in a drier boreal forest (Yoshikawa and Hinzman 2003).

The annual performance anomaly maps were validated by focusing on known disturbances such as fires. We compared changes in performance anomaly (pre- and postfire) to a field-acquired composite burn index (CBI) (Epting *et al.* 2005, Sorbel and Allen 2005). In addition, Landsat spectral indices derived from at-sensor reflectance from within a burned area and the adjacent nonburned area were compared to the performance anomaly.

Validation with CBI

We used CBI field data to assess if annual EPA captured defoliation associated with forest fires. The CBI quantifies the degree of defoliation in various canopy layers (Key and Benson 2005) and has been used to validate remotely sensed burn severity (Epting *et al.* 2005). The data were originally collected for validation and calibration for Landsat 30-m remotely sensed products, so we averaged all CBI plot data within corresponding 1 km EPA pixels. One to three additional nonburned normal-performing 1 km pixels were added for each fire and assigned a CBI of zero. Because the CBI may not be appropriate for nonforest areas (Epting *et al.* 2005), one fire was excluded because the tree cover estimate from MODIS Vegetation Continuous Fields (Hansen *et al.* 2002) had localised nonburned tree cover of less than 25%. Since EPA were not uniform within the burned perimeter prior to the fire, the difference between prefire and postfire EPA were compared to CBI.

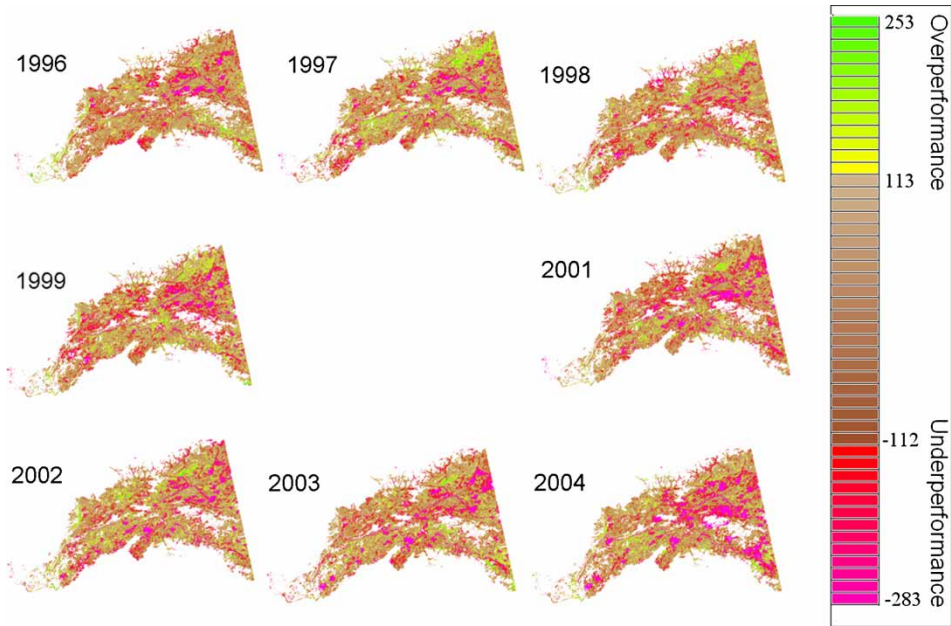


Figure 2. Boreal forest ecosystem performance anomalies in the Yukon River Basin of Alaska, 1995 to 2006. The year 2000 is excluded because the AVHRR data were unreliable.

The comparisons with field-based CBI and the change in EPA from pre- to postfire had R^2 values ranging from 0.43 to 0.75 and mean standard errors ranging from 0.21 to 0.40 (Table 2). Higher R^2 values for up to four years after the burn indicate that the EPA continues to reflect the influence of the fire. Geotz *et al.* (2006) similarly observed residual burn effects with NDVI over extended regrowth periods.

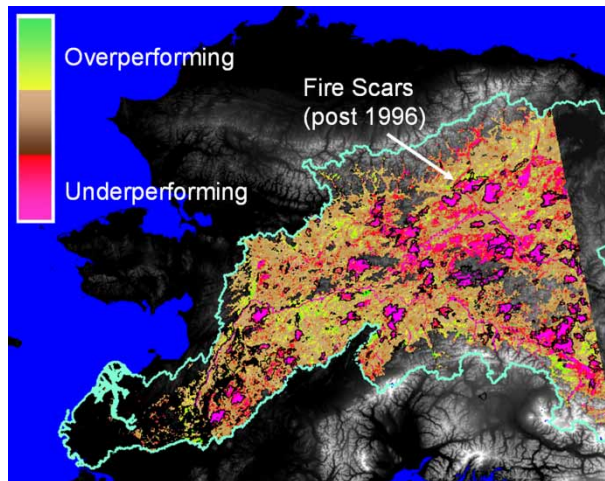


Figure 3. Ecosystem performance anomaly (EPA) for 2004, with perimeters of fires that occurred after 1996. The colored portion of the image represents the boreal forest areas of Alaska within the Yukon River Basin.

Table 2. Statistics for the regression of the composite burn index (CBI) on the difference between pre- and postfire performance anomaly at 1 km resolution for selected 2000 and 2001 fires. The fires are identified by a number and name, and the number of pixels (n) used to develop the regressions is shown.

Fire (n)	Statistic	Years			
		2001	2002	2003	2004
242 (11)	R ²	0.66	0.75	0.70	0.75
Witch fire	MSE	0.40	0.29	0.35	0.29
260 (13)	R ²	0.55	0.43	0.68	0.68
Jessica fire	MSE	0.30	0.38	0.21	0.21
288 (14)	R ²	*	0.57	0.58	0.54
Otter Creek	MSE	*	0.24	0.24	0.26

*Burned 2001

Measuring the agreement between field data and 1-km remotely sensed data is difficult because of sub-kilometre heterogeneity of vegetation, terrain, and soil. Despite this, and the fact that the original CBI data were collected for validation at the 30-m scale, the R² and MSE values indicate general agreement.

Validation using Landsat TM

Spectral indices were derived from 2006 Landsat at-sensor reflectance indices (Landsat Project Science Office 1998, Chander and Markham 2003, Chander *et al.* 2004) to compare with ecosystem anomaly data from 2004. On the year of the burn, the growing season NDVI could be confounded with early summer nonburned performance and postfire reduced performance. We used two fires to quantify the relationship between spectral indices derived from 2006 Landsat and the 2004 EPA (Table 3). Spectral indices tend to reduce the effects of different view angles and varying atmospheric conditions. The temporal dynamics of spectral indices have been useful in monitoring forest change in tropical forests (Hayes and Sader 2001). We selected vegetation indices which had some biological meaning and incorporated a diverse set of spectral bands (Table 3). The Landsat spectral indices were averaged to 1-km resolution to match the EPA pixel size and alignment. Random 1 km pixels were selected from three classes which were defined along a burn gradient using the burn perimeters and the 2004 EPA: 1) underperforming within the burn, 2) normal-performing within the burn, and 3) normal-performing from 2 to 4 kilometres outside the burn perimeter. Areas with recent burns or overperformance were excluded from the locations outside the burn perimeter. The validation tests used 123 of the 1 km pixels for the Sand Creek fire and 224 pixels for the Long Creek fire.

Agreement along the burn defoliation gradient between 2006 Landsat spectral indices and AVHRR EPA showed the strongest relationships with the specific leaf area index and the moisture index (Table 3). These two indices incorporated mid-infrared bands (band 5 or band 7), which may incorporate differences in vegetation structure (Fiorella and Ripple 1993).

Table 3. Four spectral indices are defined in terms of ratios of Landsat bands. These are applied in the analysis of the Long Creek and Sand Creek fires. Statistics (R^2) are shown for Landsat indices regressed on ecosystem performance anomaly (EPA) for 2004, as well as additional information on the fires and the Landsat images.

Index	Landsat Bands	Long Creek Fire R^2	Sand Creek Fire R^2
specific Leaf Area Index (sLAI)	$4/(3+7)$	0.71	0.72
Moisture Index	$(4-5)/(4+5)$	0.78	0.70
green NDVI (gNDVI)	$(4-2)/(4+2)$	0.58	0.49
NDVI	$(4-3)/(4+3)$	0.39	0.56
Fire information			
Fire identifier		a490	312284
Year of Burn		2002	2003
Postfire Landsat path/row		73/15	66/15
Postfire Landsat Date		5 July 2006	28 July 2006

In Figure 4, the Landsat moisture index is related to the 2004 EPA in the vicinity of the 2002 Long Creek fire, with pixels identified according to the fire gradient. The unburned normal pixels have Moisture Index values greater than 0.2, while most burned underperforming pixels have a Moisture Index less than 0.2. Normal-performing pixels within the burned area are generally between the other two classes. Both the Landsat spectral indices in 2006 and EPA in 2004 are able to represent the gradient from burned to nonburned areas. This correct gradient representation reinforces the usefulness of coarse resolution data and shows that the EPA measure is sensitive to major boreal disturbances.

Ecosystem performance anomaly trends (EPAT)

Figure 5 shows how the EPA changes with time. The map is stratified according to the direction of the anomaly trend and the significance of the slope of the regression line of the EPA with time. The areal extent of each of the categories is illustrated in Figure 6. For example, 64% of the area did not show a significant trend ($p > 0.20$). More areas had negative trends than positive trends, which was similar to trends for the entire North American boreal forest (Goetz *et al.* 2005). Negative trends were common where fires had occurred after 1998. Positive trends were commonly associated with areas which burned prior to 1995 and may represent deciduous postfire species and ultimately coniferous forest recovery (Viereck *et al.* 1992, Calef *et al.* 2005). There are ample examples of both positive and negative trend areas not associated with fires. The negative trends may represent areas of insects, disease, or changing permafrost and active layer thickness. The positive trends may indicate increasing deciduous tree components.

To validate the long-term trend of EPA, a subset area was selected where historical and recent cloud-free Landsat imagery were available, and where there was a diverse mix of decreasing and increasing EPA trends (Landsat 5 on Sept. 14, 1986, and Landsat 7 on Aug. 13, 2004, path/row 67/13). The 1 km trends map was

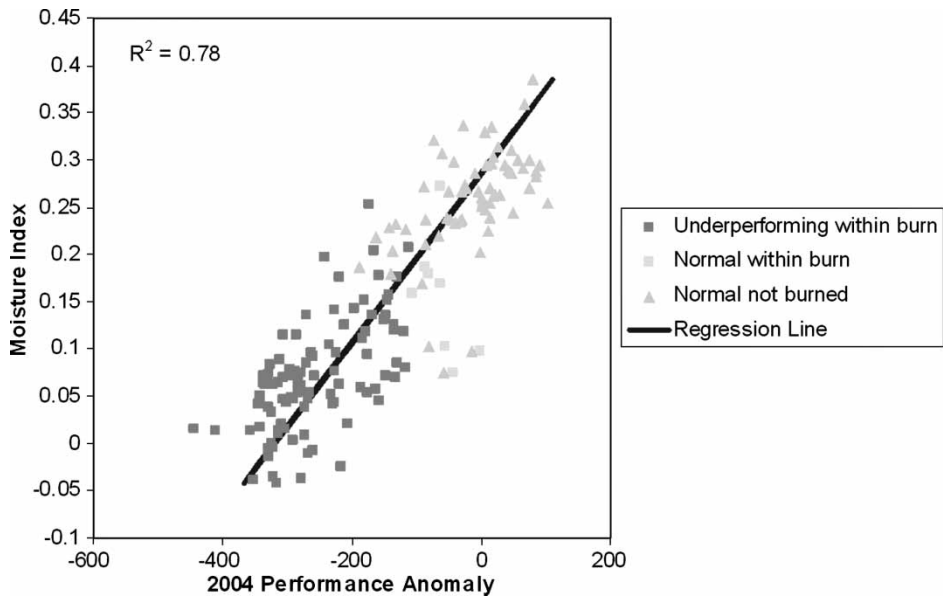


Figure 4. The relationship between the Landsat TM moisture index and the 2004 ecosystem performance anomaly at the 2002 Long Creek fire, stratified according to burn gradient classes.

categorised into four classes based on the direction and significance of the slope of the regression line: negative slopes ($p < 0.05$), positive slopes ($p < 0.05$), nonsignificant slopes ($p > 0.20$), and other (weakly significant slopes $0.05 < p < 0.20$). Random points were selected from each of the first three classes and none from the ‘other’ class. The same Landsat spectral indices used to validate the EPA (Table 3) were

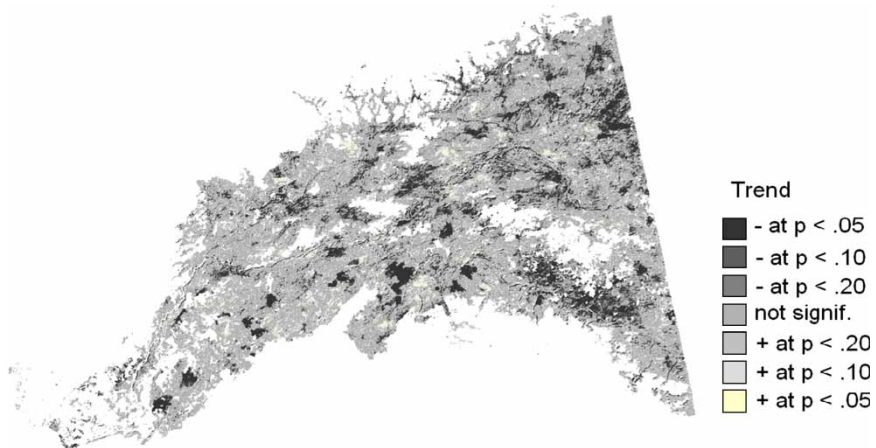


Figure 5. Ecosystem performance anomaly trends (EPAT) for the boreal forest region in the Yukon River Basin, Alaska. The image is stratified according to the direction (positive or negative) and significance (t-test probability p) of the slope of the regression line through the ecosystem performance anomaly (EPA) values and years for each pixel.

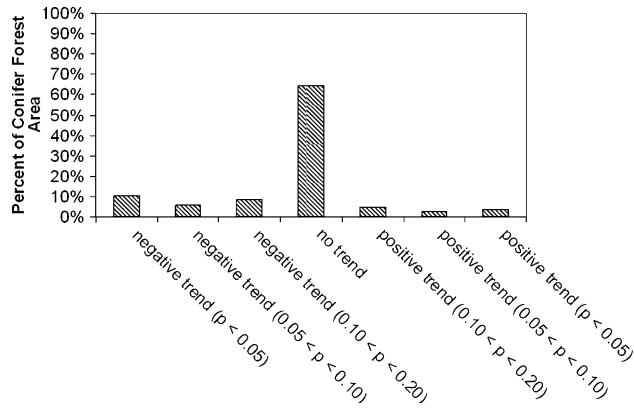


Figure 6. Percentage of each trend class in the boreal forest area, 1996 to 2004.

calculated for both of the Landsat dates and averaged to a 1-km spatial resolution. The 1986 to 2004 change in each of the four Landsat vegetation indices was calculated at the random points for each trend class.

Most of the positive trend class in the validation area was associated with a 1995 fire while most of the decreasing trend class was associated with a 1999 fire, indicating that postfire vegetation recovered during the period from 1995 to 2006. The 1995 fire occurred at the beginning of the temporal window for the trend analysis, which may explain the increasing trend in EPA. The 1999 fire occurred near the midpoint of the trend analysis window (1995 to 2004) and may have been a more severe burn, followed by drier years (2004 was a record fire year in Alaska).

All four of the Landsat spectral indices showed similar results to those shown in Figure 7 for green NDVI (gNDVI). The EPAT categories were statistically distinct in the validation data. Positive changes in Landsat spectral indices were observed in the positive trend anomaly class and negative changes in Landsat spectral indices were observed in the negative trend anomaly class. This indicates that the EPAT from 1995 to 2004 are consistent with Landsat changes in spectral indices from 1986 to 2004. The not significant class standard deviation bands overlapped zero for gNDVI and NDVI but were higher than zero for the moisture index and the specific leaf area index. Phenological differences between the September 1986 and the August 2004 Landsat scenes would affect decreasing, increasing, and nonsignificant areas similarly.

Whereas Figure 5 is based just on the slope of the regression line between the EPA measure and years, in Figure 8 the map classes were stratified by both the magnitude of the anomaly and the slope of the regression line. Positive or negative anomalies were defined when the EPA for a pixel was significant at $p < 0.1$ in 6 of the 8 years, and in the 'normal' case the EPA was not significantly different than zero at $p < 0.1$ for 3 or more of the 8 years. The three magnitude classes are intersected with three classes for the significance of the slope, to give nine map classes.

Most of the distinct blocks where the EPA magnitude is normal and the slope of the trend is negative (dark purple) were associated with fires which occurred between 1999 and 2002. This characteristic was evident in about 45 000 km² of the study area (Table 4). A few fires in 2003 and 2004 showed a similar pattern. These patterns

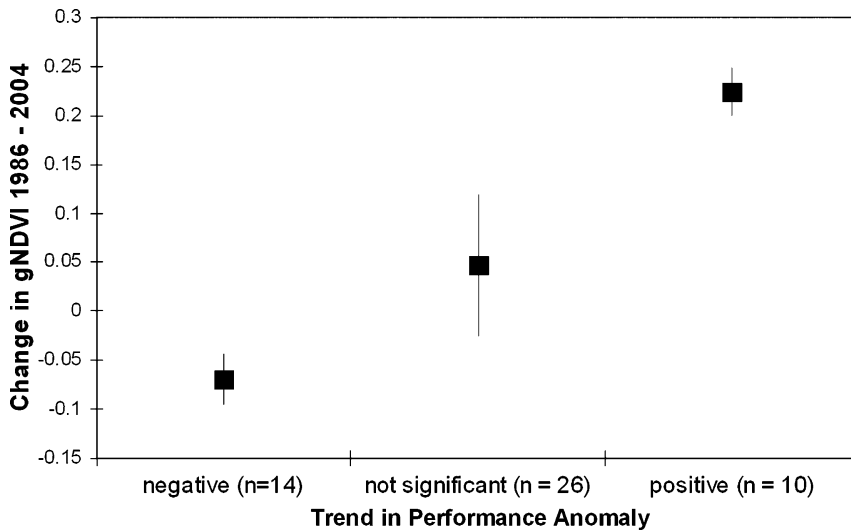


Figure 7. Long-term changes in Landsat green NDVI (gNDVI) as related to three classes of ecosystem performance anomaly trends (EPAT).

represent fires which occurred in the mid and late years of the time interval used for the trend analysis. An area along the Tanana River near the southeastern edge of the study area was normal with negative trend but was not associated with a fire.

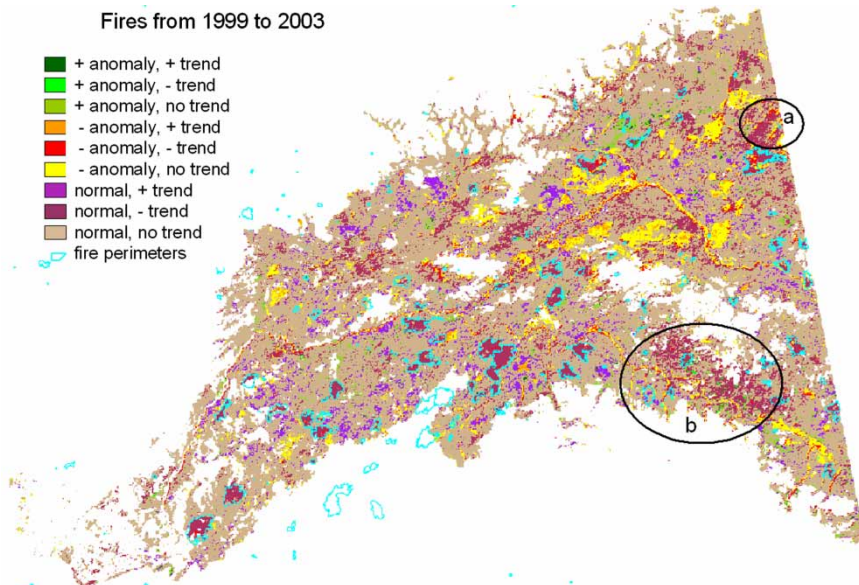


Figure 8. The ecosystem performance anomaly trends (EPAT) are grouped according to both the magnitude of the anomaly and the slope of the trend. The magnitudes are classed as positive (negative) if the EPAT is greater than (less than) zero in 6 of 8 years, and as 'normal' if it does not meet the criteria for either positive or negative. The slope of the trend is classified as positive (or negative) if it is significantly different than zero with $p < 0.10$.

Table 4. Area estimates for combinations of EPAT (trend) and EPA (performance) shown in Figure 8.

Trend performance	Positive trend: km ²	No trend: km ²	Negative trend: km ²	Total: km ²	Percentage: %
Positive anomaly	535	7140	711	8386	2.4
Normal	19208	239825	44748	303781	88.0
Negative anomaly	3363	25079	4701	33143	9.6
Total	23106	272044	50160	345310	100.0
Percentage (%)	6.7	78.8	14.5	100.0	

Negative anomalies with negative trends indicate areas under stress (red, 4 701 km²). These appear to be in areas with fires between 1999 and 2003. This class also occurs in nonburned areas along the northern part of the Alaska–Canada boundary (area a, Figure 8). This area was investigated visually with Landsat image pairs for 1986 and 2004, and widespread defoliation was evident, which may be associated with an insect or disease outbreak. Areas along the Tanana and Yukon Rivers (area b, Figure 8) tend to have a lot of negative anomalies with no trends (yellow, 25 079 km²) or negative anomalies with negative trends.

Discussion

We have developed a method of modelling ecosystem performance anomalies that can be operationally applied using current remote sensing technologies. By incorporating site potential and seasonal climate variables in the model for expected ecosystem performance, we can define management and disturbance effects in terms of the difference between the actual and expected ecosystem performance. This distinction will be helpful to land managers because measures of vegetation response such as EP are strongly influenced by the climate of a given year. The ecosystem EPA measures represent a basis for detection of changes not driven by yearly climate variations. By mapping trends in the anomalies, it is possible to identify significant disturbances such as fires, developing disturbances such as insect infestations, and more subtle disturbances such as changed soil drainage related to permafrost degradation.

Ecosystem performance

The starting point for our analysis is a measure of ecosystem performance. Although other implementations are possible, we currently use the time integrated NDVI, which is a measure of greenness that can be interpreted in terms of gross primary productivity (Bunn *et al.* 2005). These anomaly detection and mapping approaches could also be adapted to use more refined estimates of gross primary productivity (Zhang *et al.* 2007), net ecosystem exchange (Wylie *et al.* 2007), wildlife habitat, and biodiversity.

Expected ecosystem performance

The model and approach presented here provides significant advances in the application of remotely sensed data because the influences of site potential and

climate are separated from those of disturbance and land management. The direct measures of EP on an annual basis tend to combine all of these effects. The EEP measure effectively captures the spatial variation due to site potential and the temporal variation due to climate. Because the model is calibrated on relatively undisturbed areas, the influences of disturbance and land management are minimised in the EEP measure. The site potential, intuitively the maximum production expected for a site, incorporates length of growing season, aspect, slope, elevation, soil drainage, and other factors that influence boreal forest performance (Viereck *et al.* 1992, Calef *et al.* 2005).

We minimised the impacts from interpolation errors associated with the climatic data sets by using four seasonal integration periods and including elevation in the interpolation. Pavelsky and Smith (2006) found interpolated precipitation products significantly outperformed reanalysis data sets in correlations to river discharge. Hallett *et al.* (2004) found large-scale climatic data to be better predictors of ecological processes than local climate.

Chen *et al.* (2003) documented nonlinear growth in boreal forests with peak NPP occurring around a forest age of 50 years, while Goulden *et al.* (2006) found NDVI to recover 25 years after a fire. To a degree, the EEP model may adapt somewhat to age differences because piecewise regressions and regression trees can handle nonlinear relationships and because young forests were excluded from model development. In addition, with the anomaly outlier detection thresholds being based on the 90% confidence intervals, a lot of the model errors with respect to the actual EP are accounted for. The application of the EEP model was not age constrained, so there may be minor EPA errors of opposite magnitudes associated with both the lower coniferous growth rates and the higher deciduous components (which have higher NDVI values than conifer) associated with younger forest stands. The EPA values may also result in some false underperformance detection in old growth forests where NPP drops to a lower plateau at stand ages around 150 years. However, neither of these forest-age-related effects are obvious in Figure 1.

The models used current year growing season climate, except for the winter estimates which included previous year's November and December climate data. Bunn *et al.* (2005) found precipitation and temperature in the boreal forest to be driven by climatic conditions from the previous spring. High-latitude boreal forest performance was not driven by previous spring climatic conditions in their study. Given that the Yukon River Basin represents the northernmost extent of boreal forest in North America, the climate-based models developed in this study should be appropriate.

Ecosystem performance anomaly

The remaining variation, after site potential and climate are accounted for, should reveal underperforming and overperforming anomalies associated with stressed or changing boreal forest systems. We used the simple difference between EP and EEP to compute the EPA. In the boreal forest regions of the Yukon River Basin in Alaska, most of the area was not anomalous, but negative anomalies were more common than positive anomalies (Figure 6). Negative anomalies generally indicate recent fires and possible infestations of insects or disease or moisture stress related to permafrost degradation.

Trends in expected ecosystem performance anomaly

There are many potential applications for the methods to evaluate trends in ecosystem performance anomalies. To our knowledge this study is the only one that investigates anomalies in which climatic effects have been removed from the trends in boreal forests.

We expect that evaluating trends in EPA should be useful in situations similar to those where previous work has shown trends in EP to be useful. For example, remotely sensed vegetation indices at coarse resolution (greater than 250 m) can effectively track wildlife condition (Herfindal *et al.* 2006, Rasmussen *et al.* 2006), boreal forest carbon fluxes (Goulden *et al.* 2006), and fire areas (Goetz *et al.* 2006, Bartalev *et al.* 2007). Burning is the primary controller of boreal forest performance (Calef *et al.* 2005, Goetz *et al.* 2005) and is crucial for regional modelling of forest carbon sequestration variation (Magnani *et al.* 2007). Northern latitude photosynthetic activity has substantial interannual variability (Goetz *et al.* 2005) with climate having an important effect on boreal forest performance (Kang *et al.* 2005, Kimball *et al.* 2006). Decreasing trends in summer greenness were documented in the boreal forest of the Yukon River Basin (Angert *et al.* 2005, Bunn and Goetz 2006). This trend may be associated with long-term drying trends (Dai *et al.* 2004) and degrading permafrost (Jorgenson *et al.* 2006). Others have used climatic information to explain trends in remotely sensed vegetation indices (Jia *et al.* 2004, Goetz *et al.* 2005) and used climate data to map remotely sensed vegetation indices (Schwabacher and Langley 2001).

This study indicates that the boreal forests in central Alaska are responding to climatic variation in dynamic fashions which are similar to those observed in an analysis of the total North American boreal forest (Bunn and Goetz 2006). We have identified stressed boreal forest areas which may be highly vulnerable to predicted significant changes in boreal ecosystems (Rupp *et al.* 2000a, Saxon *et al.* 2005, Calef *et al.* 2005). The methods will potentially improve regional model representation of disturbances which may not be adequately represented by field data and regional models (Thompson *et al.* 2006, Magnani *et al.* 2007). Models of carbon dynamics and vegetation change will benefit from the EPAT data by identifying regions under environmental stress and vulnerable to dramatic change.

Conclusions

Our approach uses climate data to account for interannual variations in ecosystem performance. The ecosystem performance anomalies reflect ecological changes that are caused by factors other than climate or site potential. The underperforming areas documented in this study were strongly associated with burn disturbances. The results are consistent with decreasing annual trends in 8-km seasonally integrated NDVI in the Yukon River Basin as documented by Reed (2006). In portions of the study, boreal forest performance is declining faster than we would expect based on climate, and the trend is becoming more severe with time. This approach quantified localised disturbances at a 1 km resolution. Many areas with decreasing trends in EPA were associated with fires that occurred in the mid to late part of the time series; 2004 was a record fire year in Alaska. Goetz *et al.* (2005) documented decreasing trends where fires occurred late in a time series.

Increasing trends in the performance anomaly were associated with fires that occurred prior to or early in the time series, or during the first 9 years after a burn. Goulden *et al.* (2006) found that NDVI values increased for about 20 years after a fire and attributed this increase to rapid deciduous domination in the first few years postburn, with gradually increasing coniferous components after 20 years postburn.

We show that the boreal forests in central Alaska are responding to climatic variation in a dynamic fashion. The 1 km resolution input images are more detailed than those used in some previous studies. The capability to model the influences of annual climatic variation and focus on the residual anomalies offers land managers a new tool for evaluating changes on the landscape. The ecological trends that we identified are consistent with the results reported by Bunn and Geotz (2006). We have identified stressed boreal forest areas which may be vulnerable to predicted dramatic changes in boreal ecosystems (Rupp *et al.* 2000a, Saxon *et al.* 2005, Calef *et al.* 2005). The methods used in this study will potentially improve regional model representation of small patchy disturbance areas which may not be adequately represented by field data and regional models (Thompson *et al.* 2006, Magnani *et al.* 2007). We identify regionally anomalous areas so that they can be better represented in models to predict regional changes in vegetation and in carbon stocks and fluxes.

Acknowledgements

Any use of trade, product, or firm names is for descriptive purposes only and does not imply endorsement by the U.S. Government. This work was supported by the Land Remote Sensing, Geographic Analysis and Monitoring, and Earth Surface Dynamics Programs of the U.S. Geological Survey (USGS).

Notes on contributors

Bruce Wylie is an environmental scientist with the Science Applications International Corp (SAIC), contractor to the USGS Earth Resources Observation and Science Center (EROS). He received a BS in range management from the University of Montana in 1979, and his MS and PhD in range science from New Mexico State University in 1989 and 1991. Dr Wylie has developed and promoted the use of decision tree and regression tree models for spatial data. He has worked with natural resource issues and remote sensing, mapping carbon fluxes in Central Asia and the Western United States, mapping rangeland biomass in Africa and the United States Great Plains, and mapping performance anomalies in United States rangelands and boreal forest of the Yukon River Basin.

Li Zhang received a BE degree in information engineering from Wuhan Technical University of Surveying and Mapping, China, in 1998, and a MS degree in geography from South Dakota State University, USA, in 2005. From 1998 to 2003, she worked at the Chinese Academy of Surveying and Mapping, China, involved in remote sensing monitoring of urban and water resources. She is currently an environmental scientist with the Science Applications International Corp (SAIC), contractor to the USGS Earth Resources Observation and Science Center (EROS). She has been working on modelling of carbon flux, ecosystem performance, and soil moisture-vegetation index relationships. Her research interest includes the application of remote sensing, GIS, and spatial analysis of ecosystem and land-surface dynamics.

Norman Bliss received a BSc degree in Forestry from the University of California, Berkeley, a MSc degree in Forestry from the University of Washington, Seattle, and a PhD degree in City

and Regional Planning from the University of Pennsylvania, Philadelphia. He is currently a principal scientist with Science Applications International Corporation (SAIC), contractor to the U.S. Geological Survey (USGS) Earth Resources Observation and Science (EROS) Center. His research interests include understanding the stocks of carbon in terrestrial ecosystems and modelling the fluxes of carbon between the land and the atmosphere, particularly in Arctic and Boreal areas.

Lei Ji is an environmental scientist with the Science Applications International Corp (SAIC), contractor to the USGS Earth Resources Observation and Science Center (EROS). He received a BS in geoscience from Nanjing University, China, in 1982, a MS and PhD in geology from the Chinese Academy of Sciences in 1991 and 1995, and degree PhD in geography from the University of Nebraska-Lincoln, USA, in 2003. His research interests include remote sensing of land-surface characteristics and processes, spectral vegetation indices, spatiotemporal analysis of remotely sensed data, and climate-vegetation interaction. He was a recipient of the Leica Geosystems Award for Best Scientific Paper in Remote Sensing from the American Society for Photogrammetry and Remote Sensing in 2002, 2006, and 2007.

Larry Tieszen contributed to the understanding of C₃/C₄ photosynthesis and its importance in grasses and grasslands; led the development of stable isotopic applications for research in photosynthesis, WUE, land cover change, climate change, and dietary tracing; integrated research in the U.S. Tundra Biome of the IBP, and advanced interdisciplinary research and international collaboration. He assumed leadership and management responsibilities for the International Program at EROS and leads international R&D and national global change programs. He leads the integration of spatial modeling for mitigation and adaptation for climate change. These integrate satellite remote sensing (archival and real time), spatially explicit but large area carbon modelling, data assimilation techniques, and GIS to develop a quantitative understanding of the terrestrial carbon cycle.

William M. 'Matt' Jolly received a BA in Environmental Science from the University of Virginia and a PhD in Forestry from the University of Montana. He is currently an ecologist with the US Forest Service, Rocky Mountain Research Station, Fire Sciences Laboratory in Missoula, MT. His research interests center on understanding the role that weather and climate play in constraining the spatial and temporal dynamics of plant processes, particularly their relationship to plant phenology and productivity.

References

- Angert, A., *et al.*, 2005, Drier summers cancel out the CO₂ uptake enhancement induced by warmer springs. *PNAS*, 102 (31), 10823–10827. [online]. Available from: <http://www.pnas.org/cgi/doi/10.1073/pnas.0501647102> (Accessed 10/1/2007).
- Bartalev, S.A., *et al.*, 2007, Multi-year circumpolar assessment of the area burnt in boreal ecosystems using SPOT-VEGETATION. *International Journal of Remote Sensing*, 28, 1397–1404.
- Beven, K.J. and Kirkby, M.J., 1979. A physically based, variable contributing area model of basin hydrology. *Hydrological Sciences Bulletin*, 24 (1), 43–69.
- Breshears, D.D., *et al.*, 2005. Regional vegetation die-off in response to global-change-type drought. *Proceedings of the National Academy of Sciences*, 102, 15144–15148.
- Buffam, I., *et al.*, 2007, Landscape-scale variability of acidity and dissolved organic carbon during spring flood in a boreal stream network. *Journal of Geophysical Research G: Biogeosciences*, 112, G01022, doi:10.1029/2006JG000218.
- Bunn, A.G. and Goetz S.J., 2006. Trends in satellite-observed circumpolar photosynthetic activity from 1982–2003: the influence of seasonality, cover, type, and vegetation density. *Earth Interactions*, 10 (12), 1–16.

- Bunn, A.G., Goetz, S.J. and Fisk J., 2005. Observed and predicted responses of plant growth to climate across Canada. *Geophysical Research Letters*, 32, L16710, 1–4.
- Calef, M.P., *et al.* 2005. Analysis of vegetation distribution in Interior Alaska and sensitivity to climate change using logistic regression approach. *Journal of Biogeography*, 32, 863–878.
- Chander, G., *et al.*, 2004. Landsat-5 TM reflective-band absolute radiometric calibration. *IEEE Transactions on Geoscience and Remote Sensing*, 42 (12), 2747–2760.
- Chander, G. and Markham, B., 2003. Revised Landsat-5 TM radiometric calibration procedures and post calibration dynamic ranges. *IEEE Transactions on Geoscience and Remote Sensing*, 41, 2674–2677.
- Chapin, F.S. III, *et al.*, 2005. Role of land-surface changes in Arctic summer warming. *Science*, 310, 657–660.
- Chaplot, V. and Walter, C., 2003. Subsurface topography to enhance the prediction of the spatial distribution of soil wetness. *Hydrologic Processes*, 17, 2567–2580.
- Chen, J. M., *et al.*, 2003. Spatial distribution of carbon sources and sinks in Canada's forests based on remote sensing. *Tellus B*, 55, 622–642.
- Corell, R.W., 2006. Challenges of climate change: an Arctic perspective. *Ambio*, 35, 148–152.
- Dai, A., Trenberth, K.E. and Qian, R., 2004. A global dataset of Palmer drought severity index for 1870–2002: relationship with soil moisture and effects of surface warming. *Journal of Hydrometeorology*, 5, 1117–1130.
- De'ath, G. and Fabricius, K.E., 2000. Classification and regression trees: a powerful yet simple technique for ecological data analysis. *Ecology*, 8, 3178–3192.
- DeFries, R.S. and Chan, J.C., 2000. Multiple criteria for evaluating machine learning algorithms for land cover classification from satellite data. *Remote Sensing of Environment*, 74, 503–515.
- Dunn, A.L., *et al.*, 2007. A long-term record of carbon exchange in a boreal black spruce forest: means, responses to interannual variability, and decadal trends. *Global Change Biology*, 13, 577–590.
- Eidenshink, J., 2006. A 16-year time series of 1 km AVHRR satellite data of the conterminous United States and Alaska. *Photogrammetric Engineering and Remote Sensing*, 72, 1027–1035.
- Epting, J. and Verbyla, D., 2005. Landscape-level interactions of prefire vegetation, burn severity, and postfire vegetation over a 16-year period in interior Alaska. *Canadian Journal of Forest Research*, 35, 1367–1377.
- Epting, J., Verbyla, D. and Sorbel, B., 2005. Evaluation of remotely sensed indices for assessing burn severity in interior Alaska using Landsat TM and ETM+. *Remote Sensing of Environment*, 96, 328–339.
- Ferrians, O.J., 1965. Permafrost map of Alaska. *USGS Miscellaneous Investigation Series Map I-445*. Scale 1:2,500,000.
- Fiorella, M. and Ripple, W.J., 1993. Determining successional stage of temperate coniferous forests with Landsat satellite data. *Photogrammetric Engineering and Remote Sensing*, LIX (2), 239–246.
- Foley, J.A., 2005, Tipping points in the tundra. *Science*, 310, 627–628.
- Giorgi, F., 2006, Climate change hot-spots. *Geophysical Research Letters*, 33, L08707, doi:10.1029/2006GL025734.
- Goetz, S.J., *et al.* 2005. Satellite-observed photosynthetic trends across boreal North America associated with climate and fire disturbances. *Proceedings of the National Academy of Sciences*, 102, 13521–13525.
- Goetz, S.J., Giske, G.J. and Bunn, A.G., 2006. Using satellite time-series data sets to analyze fire disturbance and forest recovery across Canada. *Remote Sensing of Environment*, 101, 352–365.
- Goulden, M.L., *et al.*, 2006. An eddy covariance mesonet to measure the effect of forest age on land-atmosphere exchange. *Global Change Biology*, 12, 2146–2162.

- Hallett, T.B., et al., 2004. Why large-scale climate indices seem to predict ecological processes better than local weather. *Nature*, 430, 71–75.
- Hansen, M.C., et al., 2002. Towards an operational MODIS continuous field of percent tree cover algorithm: Examples using AVHRR and MODIS data. *Remote Sensing of Environment*, 83, 303–319.
- Harden, J.W., et al., 2000. The role of fire in the boreal carbon budget. *Global Change Biology*, 6, Suppl. 1, 174–184.
- Hassol, S.J., 2004. *Impacts of a warming Arctic, Arctic Climate Impact Assessment*, Cambridge University Press, p. 140.
- Hayes, D.J. and Sader, S.A., 2001. Comparison of change-detection techniques for monitoring tropical forest clearing and vegetation regrowth in a time series. *Photogrammetric Engineering and Remote Sensing*, 67, 1067–1075.
- Hinkel, K.M. and Nelson, F.E., 2003. Spatial and temporal patterns of active layer thickness at Circumpolar Active Layer Monitoring (CALM) sites in northern Alaska, 1995–2000. *Journal of Geophysical Research*, 108 (D2), 8168, doi:10.1029/2001JD000927.
- Herfindal, I., et al., 2006. Environmental phenology and geographical gradients in moose body mass. *Oecologia*, 150, 312–224.
- Hermann, S.M., Anyamba, A. and Tucker, C.J., 2005. Recent trends in vegetation dynamics in the African Sahel and their relationship to climate. *Global Change Biology*, 15, 394–404.
- Hicke, J.A., et al., 2003. Postfire response of North American boreal forest net primary productivity analyzed with satellite observations. *Global Change Biology*, 9, 1145–1157.
- Hinzman, L.D., et al., 2005. Evidence and implications of recent climate change in northern Alaska and other Arctic regions. *Climatic Change*, 72, 251–298.
- Jia, G.J., Epstein, H.E. and Walker, D.A., 2002. Spatial characteristics of AVHRR-NDVI along latitudinal transects in northern Alaska. *Journal of Vegetation Science*, 13, 315–326.
- Jia, G.J., Epstein, H.E. and Walker, D.A., 2004. Controls over intra-seasonal dynamics of AVHRR NDVI for the arctic tundra in northern Alaska. *International Journal of Remote Sensing*, 9, 1547–1564.
- Jia, G.J., Epstein, H.E. and Walker, D.A., 2006. Spatial heterogeneity of tundra vegetation response to recent temperature changes. *Global Change Biology*, 12, 42–55.
- Jolly, W.M., et al., 2005. A flexible, integrated system for generating meteorological surfaces derived from point sources across multiple geographic scales. *Environmental Modeling and Software*, 20, 873–882.
- Jorgenson, M.T., Shur, Y.L. and Pullman, E.R., 2006. Abrupt increase in permafrost degradation in Arctic Alaska. *Geophysical Research Letters*, 33, L02503, 1–4.
- Karlstrom, T.N., et al., 1964. Surficial geology of Alaska. *USGS Miscellaneous Geologic Investigations Map I-357*. Scale 1:1,584,000.
- Kang, S., Kimball, J.S. and Running, S.W., 2005. Simulating effects of fire disturbance and climate change on boreal forest productivity and evapotranspiration. *Science of the Total Environment*, 32, 85–102.
- Karjalainen, H., 2005. Forest restoration in Landscapes beyond planting trees. In S. Mansourian, D. Vallauri and N. Dudley, eds. *Active restoration of Boreal Forest habitats for target species*. New York: Springer, pp. 197–202.
- Key, C.H. and Benson, N.C., 2005. Landscape assessment (LA) sampling and analysis methods. *USDA Forest Service General Technical Report RMRS-GTR-164-CD*.
- Kimball, J., et al., 2006. Satellite remote sensing of terrestrial net primary production for the Pan-Arctic basin and Alaska. *Mitigation and Adaptation Strategies for Global Change*, 11, 783–804.
- Knapp, A.K. and Smith, M.D., 2001. Interannual variability in net primary production and precipitation. *Science*, 293, 1723a–1723a.
- Kronberg, B.I. and Watt, M.J., 2000. The precariousness of North American boreal forests. *Environmental Monitoring and Assessment*, 62, 261–272.

- Landsat Project Science Office, 1998, Landsat 7 science data users handbook [online]. Available from <http://landsathandbook.gsfc.nasa.gov/handbook.html> (Accessed 18 July 2007).
- Lauenroth, W.K., *et al.*, 2006. Uncertainty in calculations of net primary production for grasslands. *Ecosystems*, 9, 843–851.
- Magnani, F., *et al.*, 2007, The human footprint in the carbon cycle of temperate and boreal forests. *Nature*, 447, 848–850.
- Nowacki, G., *et al.*, 2001. Ecoregions of Alaska. USGS Open-File Report 02-297 (map).
- Pavelsky, T.M. and Smith, L.C., 2006. Intercomparison of four global precipitation data sets and their correlation with increased Eurasian river discharge to the Arctic Ocean. *Journal of Geophysical Research—Atmospheres*, 111, D21112, 1–20.
- Prince, S.D., 1991, A model of regional primary production for use with coarse resolution satellite data. *International Journal of Remote Sensing*, 12, 1311–1330.
- Rasmussen, H.B., Wittemyer, G. and Douglas-Hamilton, I., 2006. Predicting time-specific changes in demographic processes using remote sensing. *Journal of Applied Ecology*, 43, 366–376.
- Reed, B.C., 2006. Trend analysis of time-series phenology of North America derived from satellite data. *GIScience and Remote Sensing*, 43, 24–38.
- Rupp, S.T., Chapin F.S. III and Starfield, A.M., 2000a. Response of subarctic vegetation to transient climatic change on the Seward Peninsula in north-west Alaska. *Global Change Biology*, 6, 541–555.
- Rupp, S.T., Starfield, A.M. and Chapin, F.S. III, 2000b, A frame-based spatially explicit model of subarctic vegetation responses to climate change: comparison with point model. *Landscape Ecology*, 15, 383–400.
- Saxon, E., *et al.*, 2005, Mapping environments at risk under different global climate change scenarios. *Ecological Letters*, 8, 53–60.
- Schwabacher, M. and Langley, P., 2001. Discovering communicable scientific knowledge from spatio-temporal data. In *Proceedings of the Eighteenth International Conference on Machine Learning*, Williams College, 28 June–1 July [online]. Available from <http://ic.arc.nasa.gov/people/schwabac/papers.html>, (Accessed 16 July 2007).
- Smith, L.C., Sheng, Y. and MacDonald, G.M., 2007. A first pan-arctic assessment of the influence of glaciation, permafrost, topography and peatlands on northern hemisphere lake distribution. *Permafrost and Periglacial Processes*, 18, 201–208.
- Sorbel, B. and Allen, J., 2005. Space-based burn severity mapping in Alaska's National Parks. *Alaska Park Science*, Winter 2005, 1–8, [online]. Available from <http://www.nps.gov/akso/AKParkScience/Winter2005/Winter2005index.htm> (Accessed 16 July 2007).
- Striegl, R.G., *et al.*, 2005. A decrease in discharge-normalized DOC export by the Yukon River during summer through autumn. *Geophysical Research Letters*, 32(2), 1–4.
- Swets, D.L., *et al.*, 2000, A weighted least-squares approach to temporal NDVI smoothing. In *Proceedings of the 1999 ASPRS Annual Conference, From Image to Information*, Portland, Oregon, 17–21 May 1999, Bethesda: MD: American Society for Photogrammetry and Remote Sensing, CD-ROM.
- Thompson, C., *et al.*, 2006. Net carbon exchange across the arctic tundra-boreal forest transition in Alaska 1981–2000. *Mitigation and Adaptation Strategies for Global Change*, 11, 805–827.
- Tieszen, L.L., *et al.*, 1997. NDVI, C₃ and C₄ production, and distributions in Great Plains grassland land cover classes. *Ecological Applications*, 7, 59–78.
- Viereck, L.A., *et al.*, 1992. The Alaskan vegetation classification. *U.S. Forest Service General Technical Report PNW-GTR-286*, July, p. 112.
- Viereck, L.A. and Van Cleve, K., 1984. Some aspects of vegetation and temperature relationships in the Alaska Taiga. In J.H. McBeath, ed. *The potential effects of carbon*

- dioxide – induced climate changes in Alaska*. Fairbanks, AK: University of Alaska), pp. 129–142.
- Walker, G., 2007. A world melting from the top down. *Nature*, 446, 718–721.
- Wessels, K.J., et al., 2007. Can human-induced land degradation be distinguished from the effects of rainfall variability? A case study in South Africa. *Journal of Arid Environments*, 68, 271–297.
- White, A.B., Kumar, P. and Tcheng, D., 2005. A data mining approach for understanding topographical control on climate-induced inter-annual vegetation variability over the United States. *Remote Sensing of Environment*, 98, 1–20.
- Wylie, B.K., et al., 2007. Adaptive data-driven models for estimating carbon fluxes in the Northern Great Plains. *Remote Sensing of Environment*, 106, 399–413.
- Wylie, B.K., et al., 2005. Quantifying regional range condition for erosion and carbon modeling. *EOS Transactions AGU, Fall Meeting Supplement*, 86, 52, Abstract B43B-0281.
- Wylie, B.K., et al., 2003. Calibration of remotely sensed, coarse-resolution NDVI to CO₂ fluxes in a sagebrush-steppe ecosystem. *Remote Sensing of Environment*, 85, 243–255.
- Xia, C., Huang, G. and Han, A., 2005. MODIS-based estimation of biomass and carbon stock of forest ecosystem in northeast China. *Geoscience and Remote Sensing Symposium, 2005. IGARSS'05. Proceedings. 2005 IEEE International*, 4, 3016–3019.
- Yoshikawa, K. and Hinzman, L.D., 2003. Shrinking thermokarst ponds and groundwater dynamics in discontinuous permafrost near Council, Alaska. *Permafrost and Periglacial Processes*, 14, 151–160.
- Zhang, L., et al., 2007. Evaluation and comparison of gross primary production estimates for the Northern Great Plains grasslands. *Remote Sensing of Environment*, 106, 173–189.
- Zhang, L., Wylie, B.K., and Tieszen, L.L., 2006. Anomalous ecosystem performance in boreal forests of the Yukon River Basin. *EOS Transactions AGU, Fall Meeting Supplement*, 86, 52, Abstract B21A-1009.
- Zimov, S.A., Schuur, E.A.G. and Chapin, F.S. III., 2006. Permafrost and the global carbon budget. *Science*, 312, 1612–1613.